MED
T113
+Y12
7710

Correlation between optical coherence tomography variables and inter-map discrepancy in glaucoma

Maya Hasan

YALE UNIVERSITY

2011

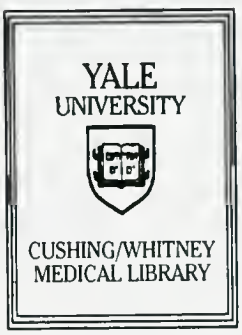
YALE
UNIVERSITY
CUSHING/WHITNEY
MEDICAL LIBRARY

Yale School of Medicine
MD Thesis Depositor's Declaration

I hereby grant to the Yale School of Medicine the non-exclusive license to photocopy, archive and make accessible, under the conditions specified below, my print and electronic thesis, in whole or in part, in all forms of media.

I agree that the Yale School of Medicine may electronically store, copy or translate my thesis to any medium or format for the purpose of preservation and accessibility. The Yale School of Medicine is not under obligation to reproduce or display my thesis in the same format in which it was originally deposited.

I retain all ownership rights to the thesis, including but not limited to the right to use in future works (such as articles and books) all or part of this thesis.

My thesis may be placed in the digital thesis repository with the following status:
(choose one only)

□ **1.** Release the entire thesis immediately for access worldwide, in perpetuity.

□ **2.** Release the entire work for Yale University access (including on-campus access and remote access) only for □ 1 year, □ 2 years, or □3 years. After this time, the work may be accessible worldwide, in perpetuity.

☒ **3.** Release the entire work for Yale University access (including on-campus access and remote access) only, in perpetuity. I understand that this thesis may be available from any Yale University computer location or authorized remote location.

I understand that descriptions of the thesis will be incorporated into library catalogs or databases. Any request to remove my thesis from the digital library repository shall be submitted in writing to the Director of the Office of Student Research. Such request shall be granted or denied at the sole discretion of the Director.

I hereby give The Yale School of Medicine the right to make available the thesis as described above.

MAYA HASAN — Name of Student

 — Signature

5/1/11 — Date

2011 — Year of Graduation

Correlation between optical coherence tomography variables and inter-map discrepancy in glaucoma

A Thesis Submitted to the

Yale University School of Medicine

in Partial Fulfillment of the Requirements for the

Degree of Doctor of Medicine

by

Maya Hasan

2011

Med
Thesis
T113
+Y12
7710

CORRELATION BETWEEN OPTICAL COHERENCE TOMOGRAPHY VARIABLES AND INTER-MAP DISCREPANCY IN GLAUCOMA. Maya A Hasan, Matthew Rosenberg, Marc Bodman, and M Bruce Shields. Department of Ophthalmology and Visual Sciences, Yale University, School of Medicine, New Haven, CT.

The purpose of this study was to identify variables measured by spectral-domain Cirrus high-definition optical coherence tomography (HD-OCT) (Carl Zeiss Meditec Inc, Dublin, CA) that were correlated with a discrepancy between retinal nerve fiber layer (RNFL) thickness and clock-hour maps, as indicators of glaucomatous damage. We hypothesized that the RNFL thickness and clock-hour maps may not always indicate the same level of glaucomatous damage and that certain variables likely influence the discrepancy.

This was a retrospective case study of glaucoma patients with Cirrus HD-OCT imaging. Discrepancies between RNFL thickness and clock-hour maps were calculated by determining the difference between assigned stages of glaucomatous damage. The means of selected variables (symmetry, signal strength, peak amplitude difference, peak horizontal deviation, and quadrant thickness) were compared between groups with discrepancies and groups without discrepancies.

Data was collected from 118 patients, including 231 eyes and 446 quadrants. Approximately 18% of quadrants demonstrated a discrepancy of $\geq$2 stages. Only the average quadrant thickness was significantly different between discrepant and non-discrepant groups.

Technological advances have provided us with increasingly higher resolution images of the optic nerve head, but no instructions regarding their utility. More research is required to determine the most clinically relevant optical coherence tomography data. Quadrant thickness measurements are correlated with discrepancies between other maps.

Acknowledgements

This thesis work would not have been possible without the guidance and support of my advisor, colleagues, friends, and family. Thanks to:

Bruce Shields for accommodating a stranger's request for help. He patiently guided me through this project and lent support at every turn. One day I hope to mentor students as he has mentored me.

Matthew Rosenberg and Marc Bodman for their efforts in this study's conception and initial data collection.

My friends for keeping me well-fed and watered – belly and soul.

My parents for their unwavering support and encouragement.

My future husband for picking me up.

Table of Contents

1 Introduction

1.1 Glaucoma

Glaucoma is a collection of diseases defined by a characteristic optic neuropathy, but with a diversity of clinical and histopathologic manifestations. There are four main classifications based on initial events: (1) open-angle glaucoma (2) angle-closure glaucoma (3) developmental glaucoma and (4) those glaucomas that are associated with other ocular and systemic disorders. The distinctive changes in the visual field and cup of the optic nerve of many glaucomas are associated with an increased intraocular pressure (IOP). These variables are the basis of current glaucoma diagnosis and treatment. Without treatment, glaucoma leads to progressive loss of the visual field and irreversible blindness. (1)

1.1.1 History

The first reference to the Greek "glaucosis" dates back to the writings of Hippocrates around 400 B.C. and referred to the bluish-green hue taken on by eyes progressively blinded by glaucoma, cataracts, or other ocular pathologies. (1) By the 10th century, the Arab physician At-Tabari had found an association with elevated IOP, but it was not until 1622 that the English ophthalmologist Richard Banister first described glaucoma in English. In the mid-19th century, German Albrecht von Graefe recognized the importance of visual field changes and appreciated the cupping of the optic nerve through the lenses of the newly-developed ophthalmoscope. (2) These initial observations identified the major factors now considered in the care of glaucoma patients, namely IOP, visual fields, and the optic nerve head. Since then, many of the technological advances made in the field have concentrated on improving quantification of these variables, and the resolution

of the optie dise in partieular.

1.1.2 Epidemiology

Glaucoma is a leading cause of global blindness, with an estimated 60 million affeeted in 2010 and almost 80 million in 2020. Approximately 8.4 million people were expeeted to be blind bilaterally from glaueoma in 2010, rising to 11.2 million in 2020. (3) Even in developed eountries, up to half of glaucoma patients remain undiagnosed, in part because the disease ean remain asymptomatie early on. (4) In 2002, the lifetime prevalenee of diagnosed glaueoma among adults in the United States was 2.0% (4 million). (5) It is the seeond most eommon cause of ambulatory visits to ophthalmologists in the United States by Medicare patients and a major expense among visual disorders. (6,7) Consistently, it has been shown that the costs assoeiated with glaucoma are proportional to its severity. (8) The prevention of disease progression is paramount to proteet both patients' vision and pocketbooks; improvements in screening and long-term management are erucial to addressing this major public health problem.

1.1.3 Natural history

Part of the diffieulty in diagnosing glaueoma is that its progression is initially silent, to patient and clinieian alike. The first, or latent, phase of glaucoma encompasses this period. In some cases the optie nerve damage during this phase oeeurs in the presenee of a rise in IOP, but both optie nerve damage and an elevated IOP ean also occur in the others' absenee. Eventually the axonal loss beeomes elinieally deteetable by visual field testing or optic nerve examination, marking the start of the second phase. However, studies show that vision loss through standard visual field testing only becomes apparent after up to 40% of the nerve tissue is lost; visual testing is further eomplieated by its

dependence on the patient's test-taking skill. Diagnosis based on evaluation of the optic nerve is also difficult to establish with an exam from only one time point; in many cases multiple visits are necessary to detect glaucomatous changes. Symptomatic patients have progressed to the third, and final, clinical phase, and inevitably go blind when given enough time and left untreated. (1)

Early diagnosis and IOP-lowering treatments therefore minimize the risk of blindness, but risk factors remain. The risk is increased in those with uncontrolled ocular hypertension, advanced stage, and ongoing progression. Patients diagnosed with glaucoma at a young age are also at increased risk of blindness because of their longer duration of disease. Early diagnosis and detection are complicated because asymptomatic patients may not seek medical care, but many patients are symptomatic at presentation; parts of this population are of lower socioeconomic status or have not been examined for a long time. Unfortunately, even those with recent ocular evaluations are not guaranteed accurate glaucoma assessment, especially those with a normal IOP Elevated IOP is an ocular risk factor, and lowering IOP is the goal of most current strategies for the medical treatment of glaucoma. It has been shown to decrease the incidence of glaucoma in randomized controlled clinical trials, and studies suggest that lowering IOP beyond a certain level may virtually stop the progression of glaucomatous damage. The efficacy of these treatments is based on their interaction with aqueous humor production and outflow pathways. (1)

1.1.4 Mechanism

A delicate balance of aqueous humor production and outflow maintains normal IOP and globe inflation (Figure 1). Aqueous humor is secreted by the ciliary epithelium and

similar in composition to protein-free plasma. It exits the eye via both the uveoscleral and trabecular pathways. Aqueous humor following the uveoscleral pathway passes between the ciliary muscle bundles, through the iris root and superchoroidal space, and into the venous system. Alternately, aqueous following the trabecular pathway is absorbed at the intersection of the uveal and corneoscleral trabecular meshworks, juxtacanalicular tissue, and Schlemm's canal. Most glaucomas are the result of decreased outflow rather than increased inflow. (9)

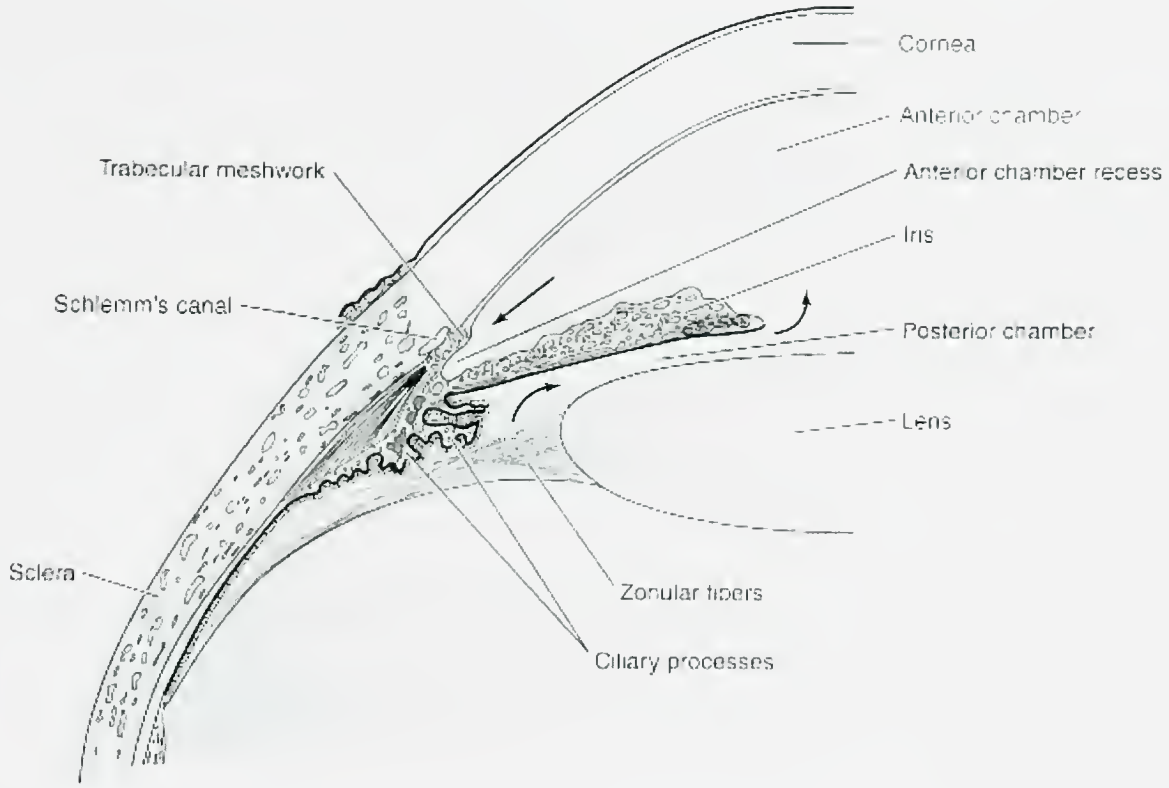

Source: Riordan-Eva P, Whitcher, JP: *Vaughan & Asbury's General Ophthalmology*, 17th Edition: http://www.accessmedicine.com

Copyright © The McGraw-Hill Companies, Inc. All rights reserved.

Figure 1. Aqueous humor production and outflow in the anterior segment. Aqueous humor is produced by the ciliary epithelium and flows out the uveoscleral and trabecular pathways. (Salmon John F, "Chapter 11. Glaucoma" (Chapter). Riordan-Eva P, Whitcher JP: Vaughan & Asbury's General Ophthalmology, 17e: http://www.accessmedicine.com/content.aspx?aID=3089104.)

Increased outflow resistance elevates IOP and can lead to glaucomatous damage of the optic nerve. In some open-angle glaucomas, particulate matter clogs the trabecular meshwork, increasing outflow resistance; in others, there are biochemical and morphological alterations to the trabecular meshwork. In angle-closure glaucomas, the iris itself obstructs outflow. Most congenital glaucomas are caused by developmental

defects in the outflow pathway. Although these glaucomas are associated with increased IOP, it is important to remember that glaucoma occurs in the setting of normal IOP as well. (9)

Glaucomatous optic neuropathy is thought to be a result of multiple pathophysiologic mechanisms. Elevated IOP is theorized to damage the optic nerve by compressing the axons of retinal ganglion cells. Ischemia is another hypothetical contributor. Damage may also result from excitotoxicity, oxidative stress, inflammatory cytokines, or aberrant immunity. Whether one trigger or many, current thinking is that glaucomatous cell death occurs by a final apoptotic pathway. Until we learn more about the processes at work in the posterior segment of the eye, our therapies will continue to target those of the anterior chamber. (9)

1.2 Optic nerve head

1.2.1 Anatomy of the optic nerve head

Glaucomatous vision loss occurs in the optic nerve head and retinal nerve fiber layer (RNFL), which contains the axons of retinal ganglion cells. These neuroepithelial cells are sandwiched between their basement membranes, or the internal and external limiting membranes, anterior to the retinal pigment epithelium. The optic nerve head has been measured with diameters ranging from at least 0.85 to 2.86 mm. (1) The optic nerve head is that part of the optic nerve that extends distally from the myelinated nerve fibers in the scleral plane to the retinal surface, while the optic disc generally refers to that part of the optic nerve head that is visible by ophthalmoscopy. Retinal ganglion cell axons from across the fundus converge to exit the globe through the lamina cribrosa, or scleral canal, which also conducts traversing blood vessels. Arcuate nerve fibers originate from the

temporal periphery and arch superiorly and inferiorly to occupy the superotemporal and inferotemporal portions of the optic nerve head that are discussed later. (1)

1.2.2 Normal optic nerve head morphology

The optic nerve head appears as a vertical oval during clinical evaluation (Figure 2). The retinal vessels entering and exiting through the lamina cribrosa are seen nasally. At the center of the disc is the depressed cup; the tissue between the two is called the neural rim. Narrow neural rims, or high cup-to-disc ratios, are commonly cited as an indicator of glaucomatous damage because retinal ganglion cell axons travel through this structure. However, multiple factors influence the actual and observed width of the neural rim, including the diameter of the optic nerve head, the contour of the cup, anatomic variation, and myopia. Both the neural rim width and the RNFL thickness appear to decrease with age, while there is conflicting data regarding whether the physiologic cup enlarges over time. Regardless, it is important to distinguish between a large physiologic cup and a large glaucomatous cup. Interocular symmetry and overall optic nerve head configuration are helpful, but it is really documented morphologic pathologic progression from normal that suggests glaucomatous optic atrophy. (1)

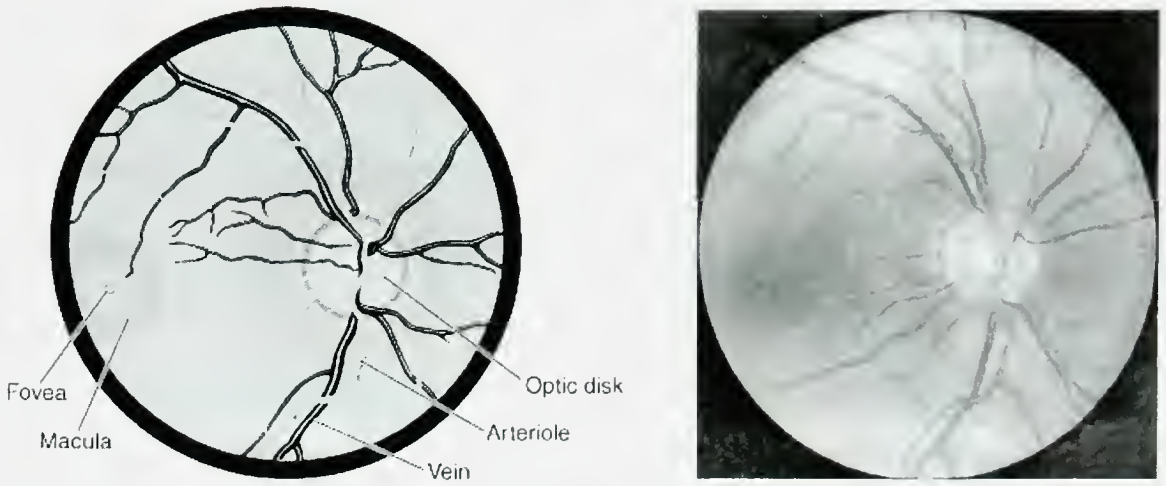

Source: Riordan-Eva P, Whitcher, JP: *Vaughan & Asbury's General Ophthalmology*, 17th Edition: http://www.accessmedicine.com
Copyright © The McGraw-Hill Companies, Inc. All rights reserved.

Figure 2. Normal optic nerve head morphology. Diagram of the fundus on the left, with corresponding photograph on the right. (Chang David F, "Chapter 2. Ophthalmologic Examination" (Chapter). Riordan-Eva P, Whitcher JP: Vaughan & Asbury's General Ophthalmology, 17e: http://www.accessmedicine.com/content.aspx?aID=3089709.)

1.2.3 Pathologic optic nerve head morphology

This pathologic progression is traced by morphologic changes in the optic disc, vasculature, and peripapillary retina (Figure 3). Focal atrophy of the optic disc usually begins with thinning of the neural rim at the vertical poles, first in the inferotemporal region, and then superotemporally. Alternately, axons of the neural rim are lost concentrically, causing the cup to appear larger while retaining its shape. If optic disc changes are allowed to progress, the neural rim eventually disappears such that the retinal vessels that once gradually rode the rim now sharply bend at the disc edge. Splinter hemorrhages of the optic disc may be the first sign of glaucoma, while tortuosity of retinal vessels usually appears during more advanced stages. Vascular changes within the

optic disc may be associated with the occlusion of retinal vessels or venous stasis, but glaucoma-related vessel narrowing can also occur beyond the edge of the disc. The peripapillary retina can show other signs of glaucomatous damage as well, with localized or diffuse RNFL defects and pigmentary disturbances. (1)

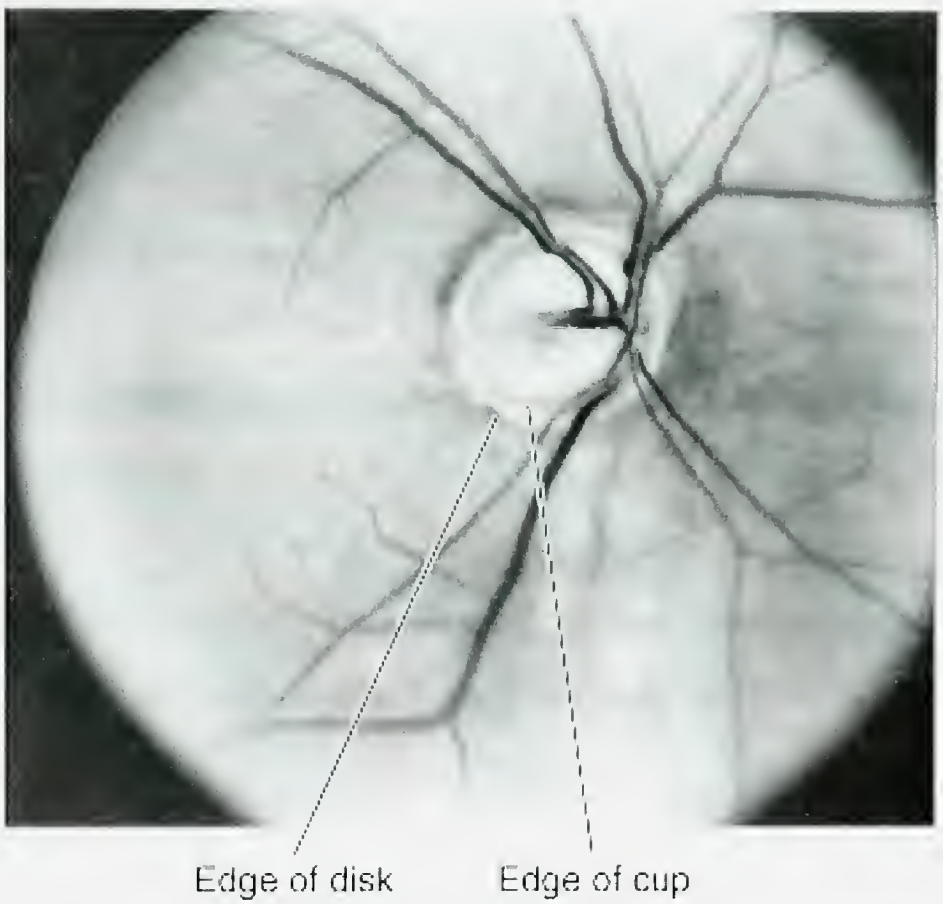

Source: Riordan-Eva P, Whitcher JP: *Vaughan & Asbury's General Ophthalmology*, 17th Edition: http://www.accessmedicine.com

Copyright © The McGraw-Hill Companies, Inc. All rights reserved.

Figure 3. Pathologic optic nerve head morphology. The neural rim is compressed between the edge of the disc and the edge of the cup in end-stage glaucoma. (Chang David F, "Chapter 2. Ophthalmologic Examination" (Chapter). Riordan-Eva P, Whitcher JP: Vaughan & Asbury's General Ophthalmology, 17e: http://www.accessmedicine.com/content.aspx?aID=3089709.)

1.2.4 Evaluation of the optic nerve head

Several techniques are currently used to evaluate the glaucomatous changes of the optic nerve head and to monitor its progressive cupping over subsequent examinations.

The modern descendent of the direct ophthalmoscope once used by von Graefe may still be used to visualize the optic nerve head, but is limited by its monocular view of a minimally magnified image. In the office, use of a slitlamp and an auxiliary fundus lens lend the benefits of stereopsis and greater magnification in inspecting the nerve head and peripapillary area, albeit with some distortion. Photographs, whether two-dimensional or stereoscopic, color or black-and-white, provide the added advantage of recording the details for later comparison during follow-up. Ultrasound can be used to detect advanced glaucomatous cupping ($\geq$ 0.7 cup/disk ratio), while measurements of retinal, choroidal, and retrobulbar blood flow relate to the pathophysiology of glaucomatous optic nerve damage. At this time, computed analysis of the optic nerve head and RNFL is gaining popularity as the technology of choice in supplementing management decisions. (1)

Such objective measurements of optic nerve head topography and pallor have undergone numerous iterations since Dr. Bernard Schwartz developed the first prototype in 1976. Many early technologies exploited the properties of stereopsis, the process by which depth is perceived from disparities between projections of the world on the two retinas. Stereophotogrammetry used these disparities to generate contour lines and maps of the optic nerve head. Stereochronoscopy detected changes between temporally-distinct images, while stereo chronometry measured these changes with a stereoplotter. Rasterstereography created a topographic map from the differential deflection of dark and light line pairs onto the disc and peripapillary retina. Techniques have also been studied to quantify optic nerve head pallor, which is indicative of neuronal atrophy. Although these instruments had clinical utility in their precision and accuracy, it was not until the development of methods to measure RNFL thickness at the turn of the century that

computed image analysis reached widespread commercial availability. (1)

Images of optic nerve topography and the RNFL changed the landscape of glaucoma diagnosis. Confocal scanning laser ophthalmoscopy produces a three-dimensional construct of the optic nerve head by translating the amount of light reflected from a series of small fundal areas into the brightness of pixels on a display monitor. Newer generations of laser tomographie seanners achieve high spatial resolution, but defining a reference plane is complicated and distinguishing damage from healthy disc by measured morphometric variables is difficult. Polarimetry exploits the changes in wave polarization as light travels through a material, and confocal scanning laser polarimetry exploits the differential retardation of light as it penetrates the birefringent RNFL to measure thickness. Reportedly high (> 80%) sensitivity and specificity, coupled with a large normative database, make the polarimeter an attractive instrument in the care of glaucoma. The retinal thickness analyzer similarly measures the RNFL thickness by calculating the distance between reflections from the internal limiting membrane and the retinal pigment epithelium. However, despite the advantages of these technologies, optical coherence tomography (OCT) has the greatest potential in the diagnosis and management of glaucoma. (1)

1.3 Optical coherence tomography

1.3.1 Technology overview

OCT is similar to ultrasonography, using light instead of sound. It is based on the principle demonstrated by the Michelson interferometer, in which the properties of electromagnetic waves are exploited in the name of scientific discovery. In instruments utilizing these interferometric techniques, a beam of light is split into a sample beam and

a reference beam. The sample beam is reflected back from media (the retina, in this case), as the reference beam is reflected back from a reference mirror. A detector measures the interference pattern of these two beams and calculates the phase difference between their paths to create a one-dimensional line of data, or an A-line, analogous to the one-dimensional line of ultrasound data called an A-scan. Two-dimensional images of the tissue are then created from a compilation of such signals. Michelson may have developed his interferometer in the late 19th century, but it took over a century for the ophthalmologic applications of directly imaging the optic nerve head and RNFL to come into view. (10)

Since inception, several generations of OCT have been produced in two families, time-domain and spectral-domain OCT, each generation with higher resolution and faster speed. Transverse resolution is dependent on A-line spacing, while axial resolution is determined in part by the light source. Both time-domain OCT and the newer family of spectral-domain instruments use diode light sources. (1) The light used in OCT is of a short wavelength so it penetrates to the retina, since it is not absorbed as well by the cornea and vitreous with their high water contents. The low-coherence light with a broad spectral bandwidth also improves resolving power. (11) As with the latest confocal scanning laser polarimeter, both the Stratus OCT (Carl Zeiss Meditec Inc, Dublin, CA) of the time-domain family and the Cirrus HD-OCT (Carl Zeiss Meditec Inc, Dublin, CA) of the spectral-domain variety come complete with large normative databases, but research is still needed regarding the utility of these instruments. For example, the Stratus OCT has been found useful in the diagnosis of glaucomatous eyes, but its role in monitoring disease progression is still unclear. Similarly, data regarding the use of spectral-domain

OCT in both the diagnosis and monitoring of glaucoma is still inconclusive. (1)

1.3.2 Time-domain versus spectral-domain OCT

Both families of instruments image the optic nerve head and measure the RNFL thickness. The Stratus OCT scans six radial lines centered on the optic nerve head and interpolates the topographic data missing from the 2 mm radius circle. The scan itself takes over one second, so microsaccades induce artifact. (10) The Cirrus HD-OCT is almost 68 times faster with a scan speed of 27,000 A-scans per second, an axial resolution of 5 μm, and a transverse resolution of 15 μm, compared to the Stratus OCT at 400 A-scans per second with a 10 μm resolution. (12) In part, spectral-domain instruments allow for higher resolution and quicker acquisition time because they rely on Fourier transformation instead of a beam splitter or reference mirror. (10) Another difference between the two technologies is the algorithm by which the RNFL is measured: Cirrus HD-OCT measures from the bottom of the nerve fiber layer, while Stratus OCT measures from the top of the ganglion cell layer. The Cirrus HD-OCT also automatically centers the scan on the optic disc by locating a dark area on the scan within a range of predetermined sizes and shapes at a break in the retinal pigment epithelium that is consistent with the optic disc. The RNFL thickness is measured in a circle of 256 A-scans with radius 1.73 mm from the center. As with instruments from previous families or generations, average RNFL measurements from the optic disc and peripapillary area are calculated per eye, per quadrant, and per clock-hour. These measurements are averages of RNFL measurements from three sequential circular scans. (12) Technical specifications are summarized in Table 1.

Table 1. Technical specifications of Stratus OCT (Carl Zeiss Meditec Inc, Dublin, CA) of the time-domain family and Cirrus HD-OCT (Carl Zeiss Meditec Inc, Dublin, CA) of the spectral-domain family. Compiled from (10) and (12).

Technical specification	**Stratus OCT**	**Cirrus HD-OCT**
Domain	Time-domain	Spectral-domain
Axial resolution	10 μm	5 μm
Scan speed	400 A-scans/sec	27,000 A-scans/sec
Light source	820 nm	840 nm

1.3.3 Clinical implications

The technological advances between time- and spectral-domain OCT do not necessarily translate into clinical improvements. For example, Leung et al. found that although Cirrus HD-OCT has lower measurement variability than the Stratus OCT, its ability to discriminate normal from glaucomatous eyes and its association with visual field testing results were not statistically different from those of the Stratus OCT. (12) Alternately, Sung et al. found that Cirrus HD-OCT had a higher sensitivity and specificity for the diagnosis of glaucoma and that the two technologies measured different RNFL thicknesses. (13) Importantly, it was established that although the measurements between the two instruments are not the same, they are correlated. (14) At this time, the clinical consequences of data generated by these technologies remain unclear.

2 Statement of purpose, hypothesis, and aims

2.1 Statement of purpose

The purpose of this study was to investigate the variables measured by the spectral-domain Cirrus HD-OCT (Carl Zeiss Meditec Inc, Dublin, CA). We aimed to identify the discrepancy between two measures of RNFL thickness as indicators of glaucomatous damage: (1) the RNFL thickness map and (2) the clock-hour map. We also aimed to evaluate variables that influence these discrepancies.

2.2 Hypothesis

The hypothesis was that the RNFL thickness and clock-hour maps may not always indicate the same level of glaucomatous damage and that certain variables likely influence the discrepancy.

2.3 Aims

- Identify the discrepancy between two measures of RNFL thickness: (1) the RNFL thickness map and (2) the clock-hour map
- Identify variables (signal strength, amplitude difference, horizontal deviation, and quadrant thickness) measured by the Cirrus HD-OCT that correlate with these discrepancies

3 Methods

3.1 Study design

This is a retrospective case study of consecutive patients with Cirrus HD-OCT imaging seen by the Glaucoma Service at the Yale Eye Center in New Haven, CT, between November 2008 and July 2009. This study was approved by the Yale University

Human Investigation Committee and conforms to the Declaration of Helsinki research on human subjects and Health Insurance Portability and Accountability Act.

3.2 Cirrus HD-OCT image acquisition

All images were acquired prior to the initiation of this study, according to the standard protocol used by the Yale Eye Center. In brief, a Cirrus HD-OCT (Carl Zeiss Meditec, Dublin, CA) with the Optic Disc Cube 200 × 200 scan pattern and Cirrus software version 3.0.0.64 was used to obtain all data. This scan pattern measures a cube with 200 data points in each dimension, covering an area of 6 × 6 mm at the optic disc. The RNFL thickness map is displayed as a blue-yellow-red color spectrum, from thinnest to thickest (Figure 4). The RNFL TSNIT normative data map and other measurements are compared to the normative database and color-coded accordingly (white > 95% of normal distribution, 5% < green < 95%, 1% < yellow < 5%, red < 1%). The software also analyzes the average thickness of each RNFL when divided into four quadrants and 12 clock-hours, as well as the symmetry between eyes (Figure 5). An experienced technician centered the scan on the optic disc to acquire the images. Scans were done with the patient seated and properly positioned. Pupils were dilated in all patients.

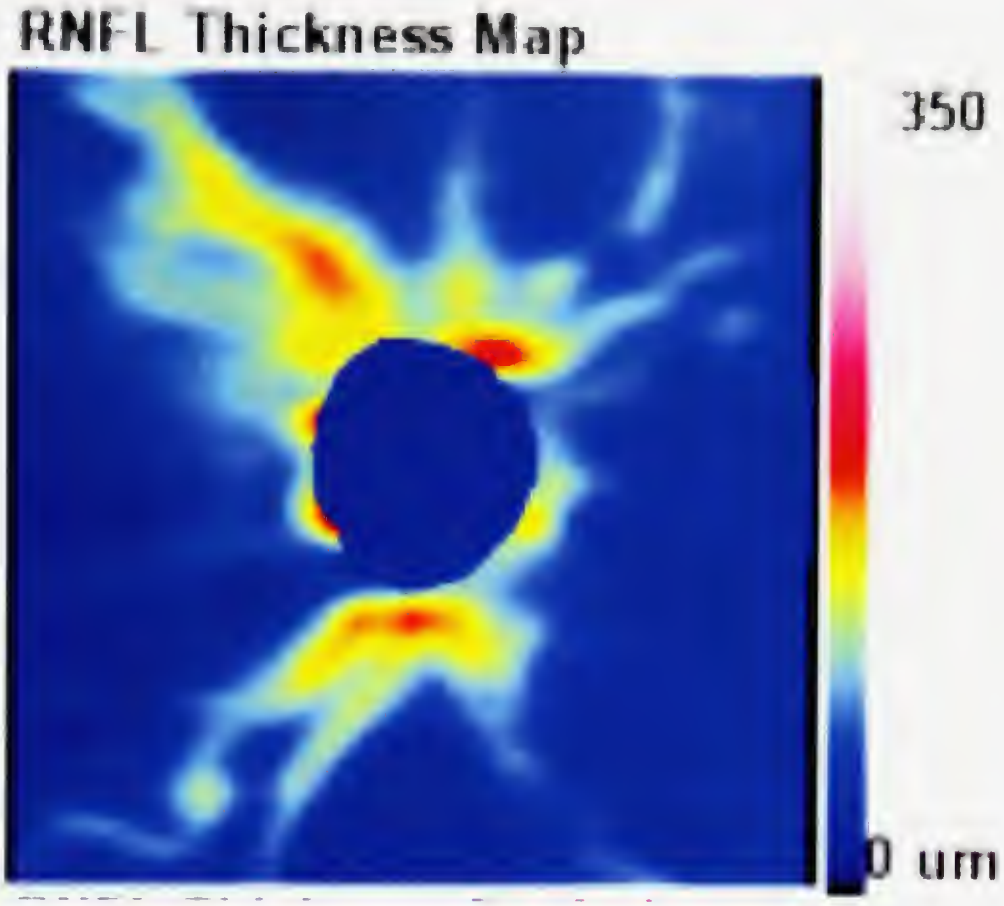

Figure 4. The RNFL thickness map, as produced by the Cirrus HD-OCT. Thickness is displayed as a blue-yellow-red color spectrum, from 0 to 350 μm.

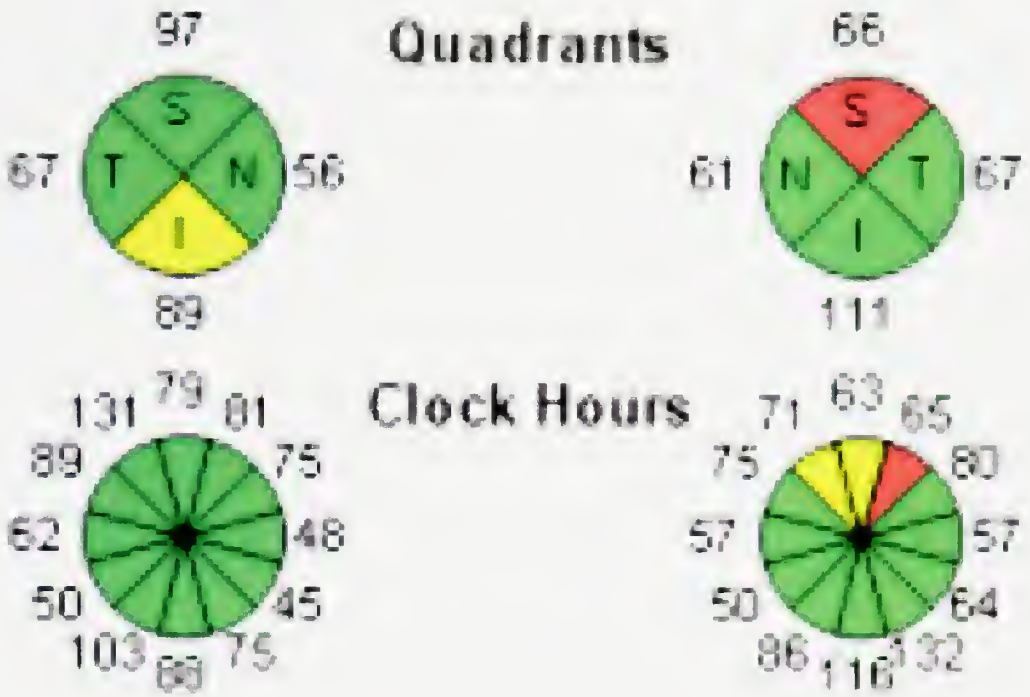

Figure 5. Quadrant and clock-hour maps. The Cirrus HD-OCT calculated the average thickness of each RNFL when divided into four quadrants and 12 clock-hours.

3.3 Data collection

3.3.1 Discrepancy determination

We determined the discrepancy, or difference, between RNFL thickness and clock-hour maps. The level of glaucomatous damage present in the superior and inferior temporal quadrants of RNFL thickness maps was evaluated, as was the damage in the same quadrants of clock-hour maps (right superior quadrant between 10 and 11 o'clock, right inferior quadrant between 7 and 8 o'clock, left superior quadrant between 1 and 2 o'clock, left inferior quadrant between 4 and 5 o'clock) because neural rim tissue is selectively lost in the superotemporal and inferotemporal regions of the optic nerve head. Each quadrant was assigned a level of damage, stage 1 through 5, as presented in Table 2. Those quadrants of the RNFL thickness map in which a clear determination of stage

could not be made were excluded from further analysis. Those quadrants of the clock-hour map with adjoining color combinations not listed in Table 2 (eg. yellow/white and red/white) were also excluded because the overall level of damage was unclear in those areas. The difference in stage between the two maps was calculated for each quadrant, and quadrants with a difference of ≥ 2 stages were considered to have a discrepancy.

Table 2. Levels of glaucomatous damage, stages 1-5.

Stage	Level of damage	RNFL thickness map	Clock-hour map
1	advanced	blue	red/red
2	moderate-advanced	blue > yellow	yellow/red
			green/red
3	moderate	yellow	yellow/yellow
4	early damage	yellow > red	green/yellow
5	normal	red > yellow	green/green
			green/white
			white/white

3.3.2 Variable compilation

Variables were compiled per patient, per eye, and per quadrant. The interocular symmetry of RNFL and signal strength were recorded. The difference in amplitude between superior and inferior peaks on the RNFL TSNIT normative data map ("amplitude difference") was measured digitally using EyeRoute software (Topcon Medical Systems, Inc., Paramus, NJ), as shown in Figure 6. The horizontal deviation between the peaks of a patient's RNFL thickness and those of the normative database,

both superior and inferior, ("horizontal deviation") was similarly calculated as described in the literature (Figure 6). (15) The average thickness of superior and inferior quadrants was also recorded for each eye from the quadrant thickness map.

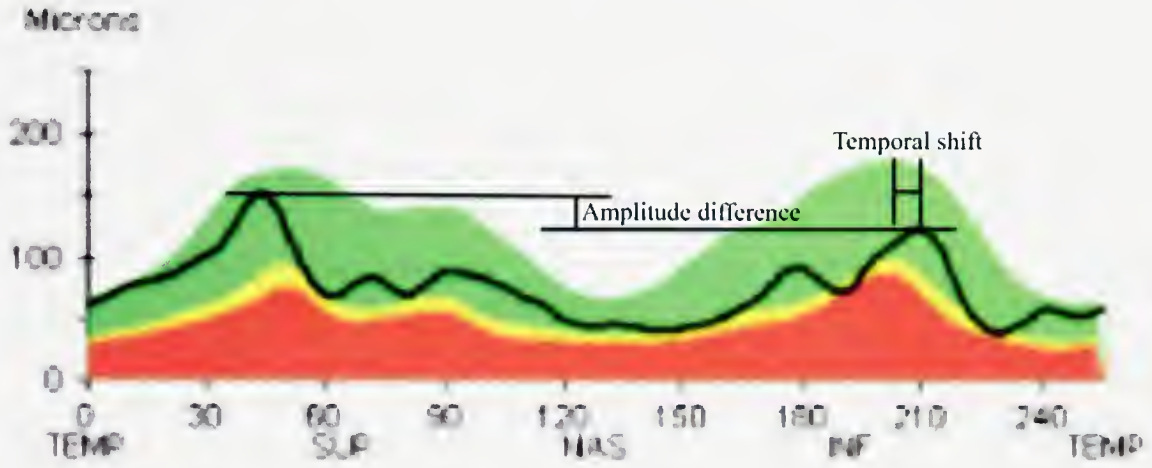

Figure 6. RNFL TSNIT normative data map with labeled variables.

Amplitude difference = superior peak – inferior peak.

Horizontal deviation = normative peak – patient peak.

3.3.3 Exclusion criteria

For those eyes scanned multiple times, a single scan was selected for analysis by excluding poor quality (e.g. blurry) images and using the "random sample of cases" function in SPSS to choose from among remaining scans. Peaks of amplitude ≤ 100 μm were excluded from amplitude difference measurements and horizontal deviation calculations because such low peaks are difficult to identify. Patients under 20 years of age were excluded from these calculations because the RNFL TSNIT (temporal, superior, nasal, inferior, temporal) normative dataset is not valid below this age. In all cases, some patients, eyes, or quadrants, were excluded from analysis because of incomplete data.

3.4 Statistical analysis

In most cases, the "compare means" function in SPSS was used for data analysis

between two groups. Data from right and left eyes were initially analyzed separately to prevent the compounding of variables. If no statistically significant difference was calculated for right eyes or left eyes, subsequent analysis considered all eyes together to determine if a difference existed with larger n. Number of observations, means, standard deviations, and P values are presented where available. Significance was set with $\alpha = 0.05$. Statistical Package for the Social Sciences version 14.0 (SPSS, Inc., Chicago, IL) was used throughout.

3.5 Credit distribution

This study was conceived by MBS and initiated with the help of MR and MB. MBS is responsible for evaluating the level of glaucomatous damage present in the superior and inferior temporal quadrants of the RNFL thickness maps. MAH evaluated the damage of the clock-hour maps, compiled the data on all other variables, and performed all statistical analysis. MBS, MR, and MAH discussed study results and conclusions.

4 Results

4.1 Study population

There were 118 patients included in this study, 67 women and 51 men. The average age was 66 ± 15 years old. Data was analyzed from 231 eyes; data was available for both eyes from 113 patients, as well as for 3 single right eyes and 2 single left eyes. Patient ethnicities were not collected due to inconsistent availability.

4.2 Discrepancy description

Of the 462 quadrants included in this study, discrepancies could only be calculated for 446 quadrants because the level of damage on clock-hour or RNFL thickness maps

could not be staged in some cases. Approximately 18% of these demonstrated a discrepancy of ≥ 2 stages. The number of quadrants per level of discrepancy is presented in Table 3.

Table 3. Number of quadrants with varying levels of discrepancy.

Quadrant	Discrepancy (|RNFL thickness map stage – clock-hour map stage|)				
	0	1	2	3	4
Right superior	35	50	20	8	0
Right inferior	46	50	11	4	1
Left superior	37	52	14	6	2
Left inferior	50	45	11	4	0

4.3 Variables per patient

4.3.1 Age and gender

Age and gender were considered as variables potentially correlated with discrepancy measurements. There were 107 patients included in this study for which discrepancy measurements were available from both eyes. Group 1a includes the 19 patients for whom two or more quadrants showed a diserepaney between RNFL thiekness and clock-hour maps, and Group 1b includes those 88 patients for which that was not the case. There was no statistical difference between the average age of patients in Group 1a and 1b (P = 0.839) (Table 4). There was also no statistical differenee between the percentage of female patients in Group 1a (57.9%) and the pereentage of female patients in Group 1b (56.8%) (P = 0.932).

Table 4. Comparison of age. There was no statistieal differenee between the mean age in patients with a discrepancy in ≥ 2 quadrants and in all other patients.

Group	Criteria	N	Mean	± SD	P value
1a	Diserepaney in ≥ 2/4 quadrants	19	64.37	16.97	0.839
1b	All others	88	65.16	14.99	

4.3.2 Symmetry

Symmetry between the RNFL thieknesses of both eyes was analyzed per patient in this study as well. As shown in Table 5, there was no statistieal differenee between the average symmetry in Group 1a and 1b (P = 0.725).

Table 5. Comparison of interoeular symmetry. There was no statistical difference between the mean interoeular symmetry in patients with a diserepancy in ≥ 2 quadrants and in all other patients.

Group	Criteria	N	Mean	± SD	P value
1a	Diserepancy in ≥ 2/4 quadrants	19	65.26	16.88	0.725
1b	All others	88	67 47	25.99	

4.4 Variables per eye

4.4.1 Signal strength

Signal strength was analyzed two ways as a variable to potentially eorrelate with the presenee of a diserepancy between RNFL thickness maps and eloek-hour maps. There were 113 right eyes and 110 left eyes for which signal strength and diserepaney

determination were both available. The average signal strength in eyes with no discrepancy in both quadrants was compared to the average signal strength in all other eyes (Table 6). There were 77 right eyes in Group 2a nd 36 right eyes in Group 2b. There was no significant difference between the average signal strengths (P = 0.125). On the left, there were 78 eyes in Group 3a and 32 eyes in Group 3b. Again, there was no significant difference in signal strength between the two groups (P = 0.771). For completeness, the analysis was then repeated considering the right and left eyes together, but the difference between average signal strengths of the two groups was still not statistically significant (P = 0.340).

Table 6. Comparison of signal strength. There were no statistical differences between the mean signal strength in eyes with no discrepancy in either quadrant and in eyes with a discrepancy in at least one quadrant.

Group	Eye	Criteria	N	Mean	± SD	P value
2a	Right	No discrepancy in either quadrant	77	7.23	1.50	0.125
2b		All others	36	7.67	1.10	
3a	Left	No discrepancy in either quadrant	78	7.27	1.28	0.771
3b		All others	32	7.19	1.47	
4a	Both	No discrepancy in either quadrant	155	7.25	1.39	0.340
4b		All others	68	7.44	1.30	

There was again no statistical difference between the average signal strength in the group with no discrepancy in both quadrants to the average signal strength in the group with discrepancy in both quadrants in either the right eye (P = 0.483) or the left eye (P =

0.648) (Table 7).

Table 7. Rigorous comparison of signal strength. There were no statistical differences between the mean signal strength in eyes with no discrepancy in either quadrant and in eyes with a discrepancy in both quadrants.

Group	Eye	Criteria	N	Mean	± SD	P value
5a	Right	No discrepancy in either quadrant	77	7.23	1.50	0.483
5b		Discrepancy in both quadrants	8	7.63	1.41	
6a	Left	No discrepancy in either quadrant	78	7.27	1.28	0.648
6b		Discrepancy in both quadrants	5	7.00	1.23	

4.4.2 Peak amplitude difference

The analyses were also performed using the amplitude difference between superior and inferior peaks on the RNFL TSNIT normative data map as the variable in question, with positive values defined as superior peak amplitude > inferior peak amplitude. The average amplitude difference in eyes with no discrepancy in both quadrants was compared to the average amplitude difference in all other eyes (Table 8). There was no significant difference in the average signal strength between groups on the right (P = 0.833) or the left (P = 0.250). There was also no statistical difference when the right and left eyes were considered together (P = 0.350).

Table 8. Comparison of amplitude difference. There was no significant difference between the mean amplitude difference in eyes with no discrepancy in either quadrant and in eyes with a discrepancy in at least one quadrant.

Group	Eye	Criteria	N	Mean	± SD	P value
7a	Right	No discrepancy in either quadrant	59	-0.23	0.56	0.833
7b		All others	28	-0.20	0.74	
8a	Left	No discrepancy in either quadrant	61	-0.28	0.53	0.250
8b		All others	24	-0.12	0.71	
9a	Both	No discrepancy in either quadrant	120	-0.26	0.54	0.350
9b		All others	52	-0.17	0.72	

As shown in Table 9, there were 59 eyes in Group 10a and 8 eyes in Group 10b; there was no significant difference in the amplitude differences (P = 0.972). On the left, there were 61 eyes in Group 11a and 5 eyes in Group 11b. In this case, the difference between average amplitude differences was significant (P = 0.028). The absolute value of the amplitude difference between superior and inferior peaks on the RNFL TSNIT normative data map was also considered. These analyses yielded similarly statistically insignificant results.

Table 9. Rigorous comparison of amplitude difference. There was no significant difference between the mean amplitude difference in right eyes with no discrepancy in either quadrant and in eyes with a discrepancy in both quadrants. There was a significant difference in left eyes.

Group	Eye	Criteria	N	Mean	± SD	P value
10a	Right	No discrepancy in either quadrant	59	-0.23	0.56	0.972
10b		Discrepancy in both quadrants	8	-0.23	1.18	
11a	Left	No discrepancy in either quadrant	61	-0.28	0.52	0.028
11b		Discrepancy in both quadrants	5	0.26	0.36	

4.5 Variables per quadrant

4.5.1 Horizontal deviation

Horizontal deviation was analyzed as another variable that could correlate with discrepancies between RNFL thickness and clock-hour maps. Deviations were arbitrarily defined as positive when the patient's peak was shifted nasally from the peak of the normative database (Table 10). There were 27 right superior quadrants with discrepancies between the two maps and 71 right superior quadrants without discrepancies; there was no statistical significance between the average horizontal deviation in both groups (P = 0.952). The same was true of similar groupings in the right inferior, left superior, and left inferior quadrants, with P values of 0.620, 0.159, and 0.418, respectively. Data from right and left superior quadrants was then combined and the data re-analyzed, but there was still no statistical difference between the horizontal deviations of superior quadrants and those quadrants with discrepancies (P = 0.376). The same held true when data from

inferior quadrants was combined (P = 0.370).

Table 10. Comparison of horizontal deviation. There were no significant differences between the average horizontal deviation in eyes with a discrepancy and in eyes without a discrepancy.

Group	Quadrant	Criteria	N	Mean	± SD	P value
12a	Right superior	Discrepancy	27	2.89	12.85	0.952
12b		No discrepancy	71	2.71	12.75	
13a	Right inferior	Discrepancy	15	1.87	12.43	0.620
13b		No discrepancy	78	0.37	10.33	
14a	Left superior	Discrepancy	21	14.11	20.57	0.159
14b		No discrepancy	74	8.29	15.29	
15a	Left inferior	Discrepancy	12	4.00	15.83	0.418
15b		No discrepancy	78	1.20	10.27	
16a	Both superior	Discrepancy	48	7.80	17.41	0.376
16b		No discrepancy	145	5.56	14.33	
17a	Both inferior	Discrepancy	27	2.81	13.80	0.370
17b		No discrepancy	156	0.78	10.28	

Horizontal deviation data was then divided into two groups for further analysis, depending on the direction of the deviation. There were 55 right superior quadrants in which the patient's peak was nasally-shifted compared to the superior peak of the normative dataset (Table 11). The average nasal deviation was not statistically different between the 15 right superior quadrants in Group 18a and the 40 quadrants in Group 18b

(P = 0.708). The same was true of the right inferior and left superior quadrants, with P values of 0.670 and 0.272, respectively. There was a significant difference in the nasal deviation between the two groups in the left inferior quadrant (P = 0.007). Results were recalculated taking the superior quadrants together and the inferior quadrants together, again with no statistically significant differences between average horizontal deviation values.

Table 11. Comparison of nasal horizontal deviation. There were no significant differences between the nasal horizontal deviation in eyes with a discrepancy and in eyes without a discrepancy, except for in the left inferior quadrant.

Group	Quadrant	Criteria	N	Mean	± SD	P value
18a	Right superior	Discrepancy	15	11.35	8.96	0.708
18b		No discrepancy	40	10.15	10.98	
19a	Right inferior	Discrepancy	7	10.84	11.96	0.670
19b		No discrepancy	35	9.40	7.21	
20a	Left superior	Discrepancy	17	19.77	18.48	0.272
20b		No discrepancy	49	14.81	14.90	
21a	Left inferior	Discrepancy	4	22.78	13.16	0.007
21b		No discrepancy	34	10.26	7.73	
22a	Both superior	Discrepancy	32	15.82	15.19	0.281
22b		No discrepancy	89	12.72	13.42	
23a	Both inferior	Discrepancy	11	15.18	13.19	0.053
23b		No discrepancy	69	9.82	7.43	

These calculations were repeated for quadrants in which the patient's peak RNFL thickness was temporally-shifted from that of the normative database, and the results are presented in Table 12.

Table 12. Comparison of temporal horizontal deviation. There were no significant differences between the temporal horizontal deviation in eyes with a discrepancy and in eyes without a discrepancy, except for in the left superior quadrant.

Group	Quadrant	Criteria	N	Mean	± SD	P value
24a	Right superior	Discrepancy	10	-9.23	8.24	0.908
24b		No discrepancy	24	-8.9	7.12	
25a	Right inferior	Discrepancy	7	-6.84	5.88	0.831
25b		No discrepancy	41	-7.32	5.40	
26a	Left superior	Discrepancy	3	-13.23	2.66	< 0.0005
26b		No discrepancy	22	-5.09	2.92	
27a	Left inferior	Discrepancy	8	-5.39	4.17	0.434
27b		No discrepancy	37	-6.91	5.07	
28a	Both superior	Discrepancy	13	-10.15	7.43	0.119
28b		No discrepancy	46	-7.08	5.80	
29a	Both inferior	Discrepancy	15	-6.07	4.91	0.470
29b		No discrepancy	78	-7.12	5.22	

4.5.2 Quadrant thickness

Quadrant thickness was also considered as an OCT variable that might be correlated

with discrepancies in RNFL thickness maps and clock-hour maps. Data was available for analysis from 113 right superior quadrants, 28 of which had a discrepancy. There was a statistically significant difference between the average quadrant thickness among those quadrants with discrepancies and those without (P = 0.004) (Table 13). The same was true for both the right inferior quadrant (P = 0.028) and the left inferior quadrant (P = 0.005), but not the left superior quadrant (P = 0.168). When data from the superior quadrants was combined, this statistical difference remained (P = 0.002), as it did when the inferior quadrants were combined (P = < 0.0005). In all statistically significant cases, the average quadrant thickness was lower among the quadrants with discrepancy.

Table 13. Comparison of quadrant thickness. There were significant differences between the quadrant thickness in eyes with a discrepancy and in eyes without a discrepancy, except for in the left superior quadrant.

Group	Quadrant	Criteria	N	Mean	± SD	P value
30a	Right superior	Discrepancy	28	80.50	13.11	0.004
30b		No discrepancy	85	94.18	23.32	
31a	Right inferior	Discrepancy	16	84.00	15.00	0.028
31b		No discrepancy	96	99.41	26.97	
32a	Left superior	Discrepancy	22	89.27	18.39	0.168
32b		No discrepancy	89	97.06	24.60	
33a	Left inferior	Discrepancy	15	81.60	13.72	0.005
33b		No discrepancy	95	102.00	27.00	
34a	Both superior	Discrepancy	50	84.36	16.09	0.002
34b		No discrepancy	174	95.65	23.96	
35a	Both inferior	Discrepancy	31	82.84	14.21	< 0.0005
35b		No discrepancy	191	100.70	26.94	

5 Discussion

5.1 Findings

The diagnosis and management of glaucoma has long been primarily based on the consideration of three factors: intraocular pressure, the visual field, and the cup of the optic nerve. Technological advances during the past several decades have provided us with increasingly higher resolutions images of the cup, but no instructions regarding their

utility. The latest software versions accompanying OCT instruments display data in a variety of ways, from absolute measurements to percentiles of a normal distribution and from measurements per eye to measurements per mieron, but eaeh is potentially misleading when taken independently. In this study we observed that there are diserepancies between the clinical impressions left by different graphs or figures from the same OCT scan, and then tried to identify other OCT variables eorrelated with these diserepaneies. Quadrant thiekness was the only variable evaluated that fulfilled this eriterion.

5.1.1 Variables per quadrant

It is possible that quadrant thiekness was eorrclated beeause it is another mcasure of thieknces, just like the RNFL thickness map and cloek hour used to caleulate diserepaney. It has been shown that the presenee of ≥1 quadrant thickness in at least thc bottom fifth pereentile of normal distribution measured by Cirrus HD-OCT has 98% sensitivity and 80% speeificity for glaucoma. (16) Other studies indicate that quadrant thiekness is useful in identifying glaucomatous eyes. (17) In general, those quadrants in whieh the determined level of glaucomatous damage did not agree between the RNFL thiekness map and the elock-hour map had a lower average quadrant height. It could be argued that the quadrant map is more similar to the eloek-hour map because it is simply an aggregate of the same RNFL thiekness values, as eompared to the normative database. If this were the case, it would be in those quadrants that the RNFL thiekness map undcrestimated the level of glaueomatous damage that the quadrant thickness was eorrelated with the prcsenee of an inter-map diserepaney. However, it may be unfair to assume that the quadrant map and elock-hour map are so similar because they were

treated differently in this study; the borders between the segments of the clock-hour map considered in this study do not align with the borders between the 4 segments on the quadrant map. It was necessary to use the superior and inferior quadrant thickness values when considering the quadrant map as a variable in order to distinguish between the superotemporal and inferotemporal quadrants for which discrepancies were calculated. It is important to remember that the superior and inferior quadrants used from the quadrant maps may be unfairly elevated because these quadrants also include more nasal, and potentially thicker, regions in and around the optic disc.

Other variables considered in this study yielded no correlation with discrepancies between the RNFL thickness map and clock-hour map. Although our study showed no association between horizontal deviation and discrepancy, previous research has shown the association between horizontal deviation and quadrant thickness. Lee and Shields also hypothesized that the horizontal deviation of RNFL thickness peaks in relation to those of the normative database with the Stratus OCT may be due to anatomic variation, scan circle misalignment, or miniscule eye movements producing imaging artifacts. (15) However, spectral-domain OCT technology, like that of the Cirrus HD-OCT used in this study, should virtually eliminate the latter two explanations. The Cirrus HD-OCT automatically centers the scan on the optic nerve head and decreased acquisition time reduces artifact. Our data show that horizontal deviations persist with this newer technology, but the questions remains if anatomic variation, such as variation in axonal patterns or blood vessel location, from the normal distribution is the sole explanation for this phenomenon. (18) Cirrus HD-OCT measures thicker values in areas of Stratus-determined thin areas and measures thinner in areas of Stratus-determined thick areas.

Knight et al hypothesized that this could be because Cirrus measures the exposed blood vessels in regions of RNFL thinning or because it measures multiple layers at once due to its decreased "smoothing" function?

5.1.2 Variables per eye

Signal strength has been reported to vary with RNFL thickness in Stratus OCT. (19) Sung et al found that there was a higher rate of poor image quality in a comparison of Cirrus HD- and Stratus OCT, while Moreno-Montañés et al found that Cirrus HD-OCT had better image quality than Stratus OCT. (13, 20) Liu et al discuss conflicting data regarding a possible positive association between average RNFL measurements and signal strength. This association has been investigated previously with similarly inconsistent results, leaving the question remaining regarding that association. (21) With many of these studies conducted using time-domain OCT, it would be interesting to gather more information regarding the effect of signal strength on spectral-domain OCT.

5.1.3 Variables per patient

Interocular symmetry has recently been investigated in normal eyes with Cirrus HD-OCT. The study found that there is a marginally significant difference in average RNFL thickness between eyes. The authors concluded that a difference exceeding 9 μm may be indicative of early glaucomatous damage. (22) It was also found that glaucomatous damage in one eye is correlated with damage in the fellow eye. (23) Unfortunately these values do not easily correspond to the "symmetry" measurement produced by OCT software.

5.2 Limitations

This was a pilot study with patients from a diverse patient population. Exclusion

criteria did not include minimal visual acuity or maximum spherical error. Data was also not collected about other ophthalmic diseases of a patient or their surgical history. Signal strength was investigated as a variable, so images with poor signal strength were not excluded, as they are in some other studies. (12) With regards to data analysis, it would be interesting to further investigate the direction in which RNFL thickness and clock-hour maps indicated different levels of glaucomatous damage. For example, does the staging of RNFL thickness maps consistently indicate a higher level of damage than the staging of clock-hour maps?

5.3 Future directions

It is important for clinicians to recognize the differences between time-domain and spectral-domain technologies, particularly between the popular Cirrus HD-OCT and Stratus OCT. There is a drive to stay up-to-date with the newest generation of instruments manufactured and the latest version of software released, but a baseline must then be re-established with each technological advance. Hopefully this study will direct future research regarding the clinical implications of quadrant height. It would be interesting to investigate whether clock-hour or RNFL thickness maps consistently indicate a more advanced level of glaucomatous damage, especially in cases where there is a discrepancy between them. Until we better understand the meaning of the data we collect, the diagnosis and management of glaucoma will remain an art of balancing intraocular pressure readings, visual field tests, and OCT results.

6 References

1. Allingham RR, Damji KF, Freedman SF, Moroi SE, Rhee DJ. Shields Textbook of Glaucoma, 6th ed. Philadelphia: Lippincott Williams and Wilkins; c2011.

2. Barnshaw HD. "Great names in the early history of glaucoma." Int Ophthalmol Clin. 1979;19(1):3-7.

3. Quigley HA, Broman AT. "The number of people with glaucoma worldwide in 2010 and 2020." Br J Ophthalmol. 2006;90(3):262-7.

4. Coleman AL. "Glaucoma." Lancet. 1999;354(9192):1803-10.

5. Ryskulova A, Turczyn K, Makuc DM, Cotch MF, Klein RJ, et al. "Self-reported age-related eye diseases and visual impairment in the United States: results of the 2002 national health interview survey." Am J Public Health. 2008;98(3):454-61.

6. Ellwein LB, Friedlin V, McBean AM, Lee PP "Use of eye care services among the 1991 Medicare population." Ophthalmology. 1996;103(11):1732-43.

7. Rein DB, Zhang P, Wirth KE, Lee PP, Hoerger TJ, et al. "The economic burden of major adult visual disorders in the United States." Arch Ophthalmol. 2006;124(12):1754-60.

8. Fiscella RG, Lee J, Davis EJ, Walt J. "Cost of illness of glaucoma: a critical and systematic review." Pharmacoeconomics. 2009;27(3):189-98.

9. Wax M, Clark A, Civan MM. "Chapter 10.3 – Mechanisms of Glaucoma." 2009. In Ophthalmology, 3rd ed. Yanoff M, Duker JS, editors. Mosby. 1008-1116.

10. Chen TC, Zeng A, Sun W, Mujat M, de Boer JF "Spectral domain optical coherence tomography and glaucoma." Int Ophthalmol Clin. 2008;48(4):29-45.

11. Jaffe GJ, Caprioli J. "Optical coherence tomography to detect and manage retinal disease and glaucoma." Am J Ophthalmol. 2004;137(1):156-69.

12. Leung CK, Cheung CY, Weinreb RN, Qiu Q, Liu S, et al. "Retinal nerve fiber layer imaging with spectral-domain optical coherence tomography: a variability and diagnostic performance study." Ophthalmology. 2009;116(7):1257-63.

13. Sung KR, Kim DY, Park SB, Kook MS. "Comparison of retinal nerve fiber layer thickness measured by Cirrus HD and Stratus optical coherence tomography." Ophthalmology. 2009;116(7):1264-70.

14. Knight OJ, Chang RT, Feuer WJ, Budenz DL. "Comparison of retinal nerve fiber layer measurements using time domain and spectral domain optical coherence tomography." Ophthalmology. 2009;116(7):1271-7.

15. Lee JC, Shields MB. "Horizontal deviation of retinal nerve fiber layer peak thickness with Stratus optical coherence tomography in glaucoma patients and glaucoma suspects." J Glaucoma. 2010;19(5):299-303.

16. Chang RT, Knight OJ, Feuer WJ, Budenz DL. "Sensitivity and specificity of time-domain versus spectral-domain optical coherence tomography in diagnosing early to moderate glaucoma." Ophthalmology. 2009;116(12):2294-9.

17. Lu AT, Wang M, Varma R, Schuman JS, Greenfield DS. "Combining nerve fiber layer parameters to optimize glaucoma diagnosis with optical coherence tomography." Ophthalmology. 2008;115(8):1352-7.

18. Ghadiali Q, et al. "An analysis of normal variations in retinal nerve fiber layer thickness profiles measured with optical coherence tomography." J Glaucoma. 2008;17(5):333-40.

19. Wu Z, Huang J, Dustin L, Sadda SR. "Signal strength is an important determinant of accuracy of nerve fiber layer thickness measurement by optical coherence tomography." J Glaucoma. 2009;18(3):213-6.

20. Moreno-Montañés J, Olmo N, Alvarex A, García N, Zarranz-Ventura J. "Cirrus high-definition optical coherence tomography compared with Stratus optical coherence tomography in glaucoma diagnosis." Invest Ophthalmol Vis Sci. 2010;51(1):335-43.

21. Liu Y, Samarawickrama C, Pai A, Tariq Y, Mitchell P. "Stratus OCT signal strength and reliability of retinal nerve fiber layer measurements." Am J Ophthalmol. 2010;149(3);528-9.

22. Mwanza JC, Durbin MK, Budenz DL. "Interocular symmetry in peripapillary retinal nerve fiber layer thickness measured with the Cirrus HD-OCT in healthy eyes." Am J Ophthalmol. 2011;Epub ahead of print.

23. Bertuzzi F, Hoffman DC, De Fonseka AM, Souza C, Caprioli J. "Concordance of retinal nerve fiber layer defects between fellow eyes of glaucoma patients measured by optical coherence tomography." Am J Ophthalmol. 2009;148(1):148-54.

YALE MEDICAL LIBRARY
3 9002 07932 1890

HARVEY CUSHING/JOHN HAY WHITNEY MEDICAL LIBRARY

MANUSCRIPT THESES

Unpublished theses submitted for the Master's and Doctor's degrees and deposited in the Medical Library are to be used only with due regard to the rights of the authors. Bibliographical references may be noted, but passages must not be copied without permission of the authors, and without proper credit being given in subsequent written or published work.

This thesis by
has been used by the following person, whose signatures attest their acceptance of the above restrictions.

NAME AND ADDRESS **DATE**